In situ developed laminates with large microstructural differences between layers of similar composition

SALVADOR BUENO, CARMEN BAUDÍN
Instituto de Cerámica y Vidrio, CSIC. Campus de Cantoblanco, 28049, Madrid, Spain

Published online: 21 April 2006

Fabrication of alumina-aluminium titanate laminates that combine high strength external layers with flaw tolerant internal layers is limited by the difficulty of the co-sintering of layers with large differences in the green state. This work describes a new method to obtain alumina-aluminium titanate layered materials constituted by layers with large differences in terms of grain size starting from green bodies with similar microstructures. The approach is based on the effect of small amounts of titania (TiO_2) as agents for alumina grain growth enhancement. Starting from a fine grained green body that combined alumina layers with composite layers made of mixtures of alumina and titania, a two step sintering schedule led to a layered structure with external layers of small grain sized alumina combined with internal alumina layers with large grain size due to the diffusion of titanium. The large grain sized alumina layers conferred flaw tolerant behaviour to the laminate due to crack branching and bridging.

1. Introduction

Ceramic oxides present very attractive properties for structural applications at high temperatures such as hardness and chemical inertness, but lack reliability due to the brittle fracture mode. In the past, much of the effort to improve the mechanical behaviour of ceramics was placed in producing the highest degree of homogeneity in bulk monophase ceramics with very small flaws. However, in the last two decades new strategies fundamentally different from the conventional "flaw elimination" approach of monolithic ceramics have emerged directed to achieve "flaw tolerance". Advances in processing technology have made it possible to mimic the approach used by nature to design structures, such as shells and teeth, in which the layered architecture combining materials with different properties leads to a laminate with mechanical behaviour superior than those of the individual constituents [1].

In general, ceramic laminates are designed on the basis of the mechanical and thermal properties of monoliths with the same composition of the layers and processed using the same green processing route and sintering schedule as that of the laminate. This approach assumes that no interactions between the different layers take place at the interfaces during sintering, as occurs when micron-sized particles of compatible phases are used to fabricate the laminate.

Alumina (Al_2O_3)—aluminium titanate (Al_2TiO_5) composites present flaw tolerance due to toughening mechanisms associated with the thermal expansion mismatch between alumina and aluminium titanate [2–5]. For similar thermal treatments, composites with high aluminium titanate contents present high flaw tolerance but low strength whereas high strength is limited to low or no second phase additions. Moreover, lower thermal expansion and Young's modulus values are associated with higher aluminium titanate contents. Therefore, when only composition is considered as variable for a laminate design with high strength external layers combined with flaw tolerant internal ones, tensile residual stresses develop in the external layers thus limiting strength [6].

One possibility for laminate design combining high strength and toughness is that initially proposed by An et Chan [7–8], in which microstructural elements are designed to provide fundamentally different mode of crack control. The basic idea is to alternate ceramic layers with homogeneous microstructures, designed for hardness and wear resistance, and heterogeneous microstructures, designed for toughness and damage dispersion. Main requirement for such systems is that the different layers could be sintered to high density under the same conditions, with low elastic and thermal mismatch [8]. In the alumina-aluminium titanate system, Russo et al. [9]

0022-2461
DOI: 10.1007/s10853-006-6088-8

proposed to combine high strength surface layers consisting of homogeneous mixtures of alumina with low aluminium titanate contents with high fracture energy internal layers of the same composition with heterogeneous microstructure. As the thermal expansion behaviours of layers with the same composition are similar, such laminates are free of residual stresses. The limit of this approach is the difficulty to obtain constituent layers of the same composition with large microstructural differences, and, therefore, with significant differences in the mechanical behaviour, because it implies the co-sintering of layers with large differences in the green state.

In this work, a new way is proposed to obtain laminates with large microstructural differences between contiguous layers. This approach is based on the effect of small amounts of titania (TiO_2) as agents for alumina grain growth enhancement [10]. The proposed structure is constituted of high strength external layers of small grain sized alumina combined with flaw tolerant internal layers. In the green state, alumina layers are combined with composite layers made of mixtures of alumina and titania. A two step sintering schedule is designed in order to obtain co-sintered layers of very different microstructures. An isothermal treatment at a temperature (1200°C) lower than that of aluminium titanate formation, 1280°C [11], is proposed for initial co-sintering of the layers. A subsequent high temperature (1550°C) isothermal treatment is proposed to promote alumina grain growth as well as full densification and reaction between alumina and titania to form aluminium titanate in the internal layers and thus, equilibrium in the material. In principle, titanium diffusion might take place during the whole thermal cycle but would be more extensive at high temperatures, once initial co-sintering of the layers has taken place.

The main hypothesis of the work is that interlayers of large grain sized alumina would be formed between the alumina and the composite layers due to the effect of titania. As the microstructural heterogeneity is developed during sintering, no decohesion of the layers due to differential sintering is expected. The focused material would present high strength, provided by the external fine grained alumina layers, combined with the desirable behaviour of large grained alumina materials in terms of flaw tolerance, provided by the *"In situ"* formed internal alumina layers [12]. Besides, due to the similarity between the thermal expansions of the layers, negligible residual stresses are expected to develop in this system.

An alternate way to reach a similar structure with alternate large and fine grained alumina layers would be to combine undoped alumina layers with others doped under the solubility limit in the green state. This approach was not used due to two main reasons. On one hand, the difficulty that implies to reach highly homogeneously dispersed slurries of alumina with very low titania amounts, that would lead to heterogeneities and aluminium titanate formation in the sintered material as occurred in other alumina materials doped with titania under the solubility limit [13]. On the other, the large differences existing between shrinkage during the initial sintering stages of undoped alumina and alumina doped with very small titania amounts, that would impede the co-sintering of the layers.

2. Experimental

The starting materials were commercial Al_2O_3 (Condea, HPA05, USA) and TiO_2 (Merck, 808, Germany) powders. Al_2O_3 purity was 99.9 wt.% with Fe_2O_3 (0.05 wt.%) and K_2O (0.04 wt.%) as main impurities. SiO_2 and Na_2O contents were 0.02 wt.% and 0.006 wt.%, respectively. TiO_2 purity was 99.1wt.% with P_2O_5 (0.4 wt.%) as main impurity, no Na_2O and 0.03 wt.% SiO_2 content. A mixture of Al_2O_3 (95 wt.%) and TiO_2 (5 wt.%) was used to obtain the sintered composition with 10 vol.% of aluminium titanate.

Stable suspensions of the single oxide and the mixture were prepared using the optimum conditions established in a previous work [4]. First, the powders were dispersed in deionised water by adding 0.5 wt.% (on a dry solids basis) of a carbonic acid based polyelectrolyte (Dolapix CE64, Zschimmer-Schwarz, Germany). Suspensions were prepared to a solids loading of 50 vol.% and ball milled with Al_2O_3 jar and balls during 4 h. Plates of $70 \times 70 \times 10$ mm^3 of the monoliths and the laminate were obtained by slip casting and dried in air. The laminated structure in the green state was formed by five layers, the outer layers (width $\cong$ 2500 μm) and the central layer (width $\cong$ 1500 μm) made of alumina and the two inner layers (width $\cong$ 330 μm) made of the alumina + titania mixture. Layer dimensions were calculated, from the casting kinetics curves and the sintering shrinkage of the monoliths to reach a layered structure, after machining, with external and central alumina layers of width $\cong$ 1300 μm and internal alumina/aluminium titanate composite layers of width $\cong$ 300 μm, as described elsewhere [6]. Sintering of the green plates was performed in air in an electrical box furnace (Termiber, Spain) at heating and cooling rates of 2°C min^{-1}, with a 4 h dwell at 1200°C and a 3 h dwell at 1550°C. For all tests, samples were diamond machined from the sintered blocks.

Microstructural characterisation was performed by scanning electron microscopy (SEM, Zeiss DSM 950, Germany) on polished and thermally etched (1500°C during 2 min) or chemically etched (HF 10 vol% - 1 min) surfaces. The average grain size was determined by the linear intercept method [14] considering at least 200 grains for each phase.

The profiles of titanium were determined by wavelength dispersive X-ray spectrometer, WDS, (JEOL, Superprobe JXA-8900 M, Japan) on polished cross surfaces of the laminate, operating at 15 kV, 20 nA and 10 s in the peak position. The *k*-factors in the quantification were calculated using the atomic number (*Z*)-absorption-fluorescence (ZAF) correction. The analysis was made

TABLE I Properties of the monolithic materials for the laminate design

	α_{25-850} 10^{-6} ($^{\circ}C^{-1}$)	E (GPa)
A	8.2 ± 0.1	388 ± 5
A10AT	7.8 ± 0.1	349 ± 4

A: Alumina, A10AT: Alumina + 10 vol.% Aluminium titanate, α_{25-850}: average thermal expansion coefficient between 25 and 850°C, E: Young's modulus.

TABLE II Grain size of the studied materials

		G_A (μm)	G_{AT} (μm)
Monoliths	A	5.5 ± 0.5	–
	A10AT	3.9 ± 0.3	2.4 ± 0.2
Laminate	Central areas of the A layers	5.3 ± 0.4	–
	Central areas of the A10AT layers	3.9 ± 0.3	2.3 ± 0.2

A: Alumina, A10AT: Alumina + 10 vol.% Aluminium titanate, G: grain size.

along three straight lines perpendicular to the layers, taking spots with 5 μm diameter.

For thermal expansion coefficients, the thermal expansion curves of pieces of $10 \times 5 \times 5$ mm^3 on heating (5°C min^{-1}) were recorded in a differential dilatometer (402 EP, Netzsch, Germany) and corrected for the system expansion. The average thermal expansion coefficients between 25 and 850°C were calculated for three samples of each composition; given results are the average of the determinations and errors are the standard deviation.

Dynamic Young's modulus was determined from the resonance frequency of bars ($4 \times 6 \times 50$ mm^3) in bending (Grindosonic, J.W. Lemmens, Belgium). Single-Edge-V-Notch-Beams of $4 \times 6 \times 50$ mm^3 of the monoliths and the laminate were tested in a three point bending device using a span of 40 mm and cross head speed of 0.005 mm · min^{-1} (Microtest, Spain). The notches were initially cut with a 150 μm wide diamond wheel to a depth of about 70% of the final depth. Using this slot as a guide, the remaining part of the notch was done with a razor blade sprinkled successively with a 6 μm and 1 μm diamond paste. The depth of the notches, a, was approximately 0.85 mm ($a/w \cong 0.14$, w = height of the sample) which resulted in a relation $a/w_A \cong 0.4$ for the width of the external alumina layer, w_A, in the laminated samples. The tip radii of the notches were optically observed to check that they were below 30 μm. The curves load versus displacement of the loading frame were recorded during three tests for each material. The crack path in the notched samples was characterized by optical microscopy of the polished lateral faces.

3. Results and discussion

The properties of the monoliths of interest for the laminate design are summarised in Tables I and II. These monoliths had homogeneous microstructure (Fig. 1a–b); reaction between alumina and titania was complete in the composite at SEM and XRD [4] levels and aluminium titanate was homogeneously distributed and located mainly at alumina triple points and grain boundaries (Fig. 1b). The lack of significant differences between the thermal expansion coefficients (Table I) assured the feasibility of a laminate combining the two compositions with negligible residual stresses due to differences between the thermal expansions of the layers. Therefore, a laminate with external alumina layers would present strength values similar to those of alumina, and higher than those of the alumina-aluminium titanate composite.

The microstructure of the sintered laminate made from a green structure consisting of two external and one central alumina layers and two alumina + titania internal layers is shown in Fig. 2a–d. The different colours that appear at low magnification (Fig. 2a–b) reveal that the thermal

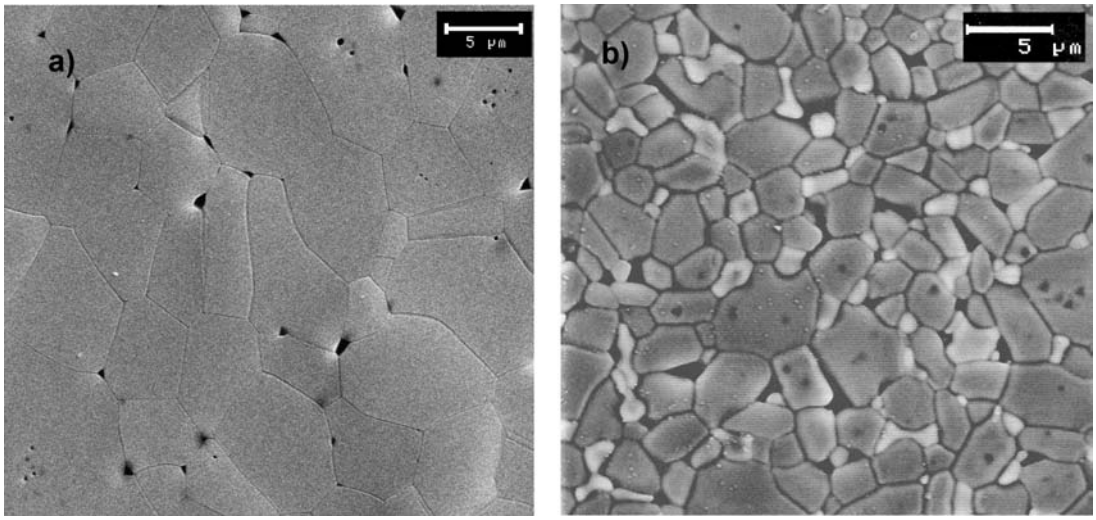

Figure 1 Characteristic microstructures of the monolithic materials. Scanning electron micrographs of polished and thermally etched (1500°C-2 min) surfaces. (a) Alumina and (b) Alumina + 10 vol.%aluminium titanate (A10AT).

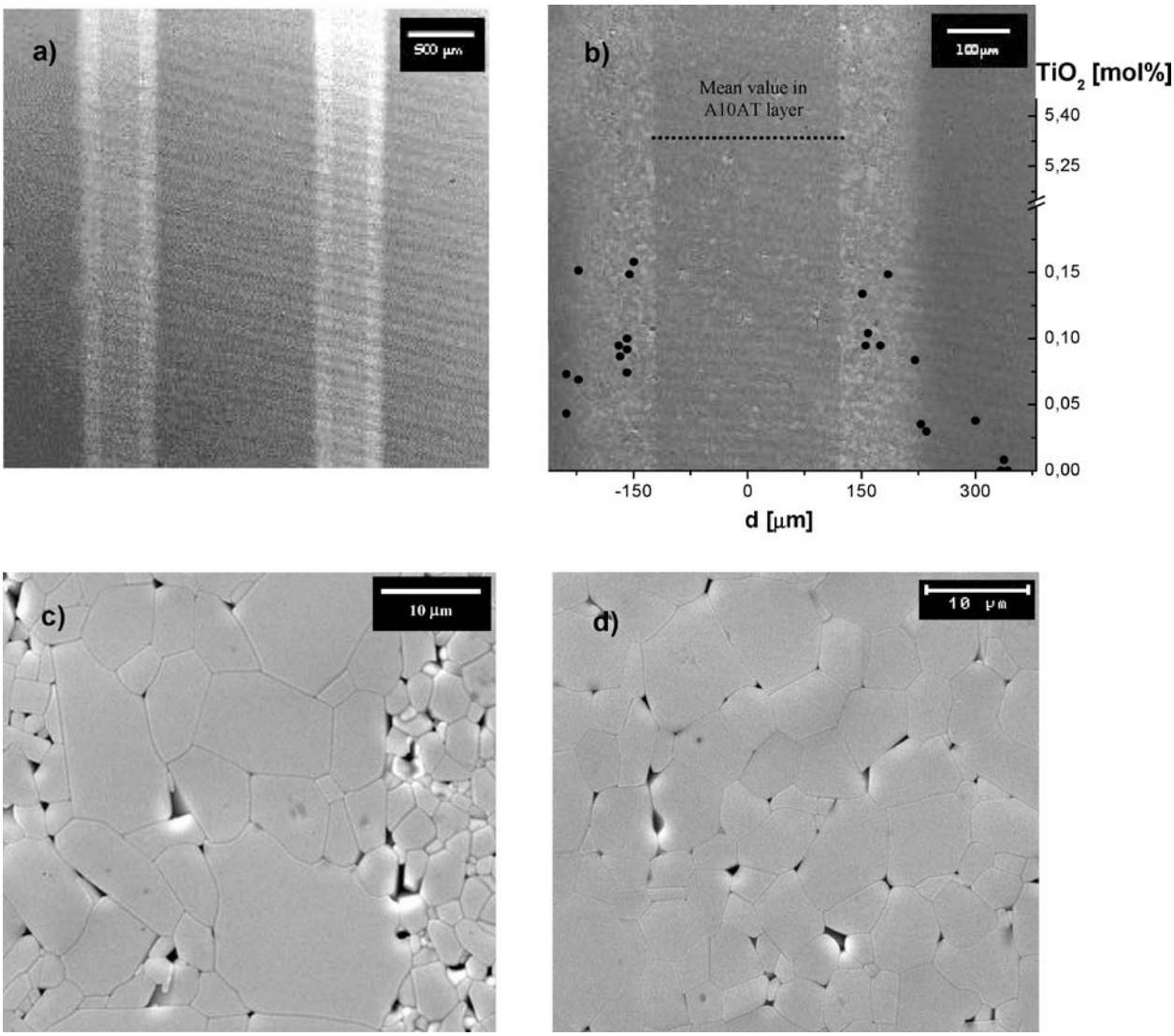

Figure 2 Characteristic microstructures of the laminated materials. Scanning electron micrographs of polished surfaces. Thermally (c, d; 1500°C-2 min) or chemically (a, b; HF 10 vol% -1min) etched surfaces. (a) Low magnification micrograph of the laminate. The complete structure is observed: two external and one central layers of fine grained alumina (dark grey), two internal layers of alumina + 10 vol.% Aluminium titanate (intermediate grey) and four layers of large grain sized alumina (clearest grey) contiguous to the composite layers. (b) Detail of a composite layer with the large grain sized alumina layers at both sides. The profile of TiO_2 content in the alumina layers determined by wavelength dispersive X-ray spectroscopy analysis is shown. (c) Interface between a composite layer (right) and the contiguous large grain sized alumina layer (left). Alumina (dark grey) and aluminium titanate (clear grey) are observed in the composite layer. (d) Central part of the alumina layers in the laminate.

treatment led to a laminate constituted by nine layers and not by the original five. Two additional layers (light grey), of about 150 μm width, are observed located at each side of the internal composite layers.

The additional layers had extremely bimodal microstructures, in terms of grain sizes, as those reported for Ti-doped aluminas [10], constituted mostly by very large (maximum dimension up to 20–25 μm, Fig. 2c) and irregularly shaped grains surrounding groups of small ($\cong$2–3 μm) alumina grains whereas the external and central alumina layers (Fig. 2d) as well as the internal composite layers (Fig. 2c) presented microstructures similar to those of the corresponding monoliths (Fig. 1a–b), with the same average grain sizes (Table II).

Fig. 2b shows that significant Ti amounts were found at both sides of the composite layers through the whole widths ($\cong$150 μm) of the contiguous large grained alumina layers. The fact that similar profiles were found at both sides of the two composite layers indicated that the presence of Ti was due to diffusion during the thermal treatment, and not to sedimentation processes during green processing. Therefore, titanium diffusion during sintering originated the four additional layers with exaggerated alumina grain growth during sintering, leading to the desired layered structure with contiguous alumina layers with the same phase composition and extremely different microstructures (Fig. 2c–d). The presence of some elongated grains in the large grained alumina layers might be attributed to the action of liquid formed by localised amounts of SiO_2, Na_2O and TiO_2, as reported by other authors [13, 15]. These grains were scarcely observed, and always very close to the composite layers, due to the low

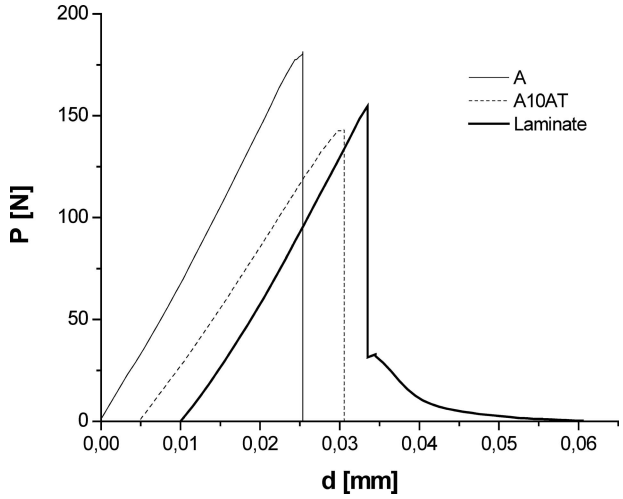

Figure 3 Characteristic load-displacement curves of notched samples of the laminate and the monoliths with a relationship between the notch depth and the height of the sample of 0.14. Crack arrest and further stable growth is observed for the laminate. The origins of the curves for A10AT and the laminate have been moved to differentiate the curves.

impurity contents of the starting powders (0.1–0.5 wt.%) with small amounts of the above mentioned compounds ($\leq$0.03 wt.%).

In Fig. 3, characteristic load-displacement curves of notched samples of the laminate and the monoliths are shown. After fracture initiation, the load plummeted for all monolith samples, indicating unstable crack propagation through their whole height. Conversely, after dropping down to approximately one third of the total load bearing capacity of the laminate samples, the load decreased smoothly for increasing displacement indicating that crack arrest and stable propagation occurred. Both parts of the layered samples remained together after testing.

The mechanisms for crack arrest and further stable propagation in the layered structure can be derived from the crack path in the fractured samples (Fig. 4), in which the large alumina grains of the layers formed *"In situ"* were clearly observed acting as sites for crack branching (Fig. 4a), as the crack entered the large grained alumina layer, and bridges (Fig. 4b) in the wake of the propagating crack. Most grains found in this material acting as crack diverting sites were not elongated, as observed in Fig. 4, revealing that the capability of the large grained alumina layer for crack branching and bridging relies on the presence of large grains ($\cong$60–80 μm), and not on the presence of grains with high aspect ratio aligned normal to the mean direction of crack propagation, as observed in other alumina-based laminates [7, 8, 16].

4. Conclusions

The adequacy of a new way to fabricate laminates with large microstructural differences between contiguous layers, starting from green structures with similar microstructures in the system Al_2O_3-TiO_2, has been proved. In particular, internal large grain sized alumina layers,

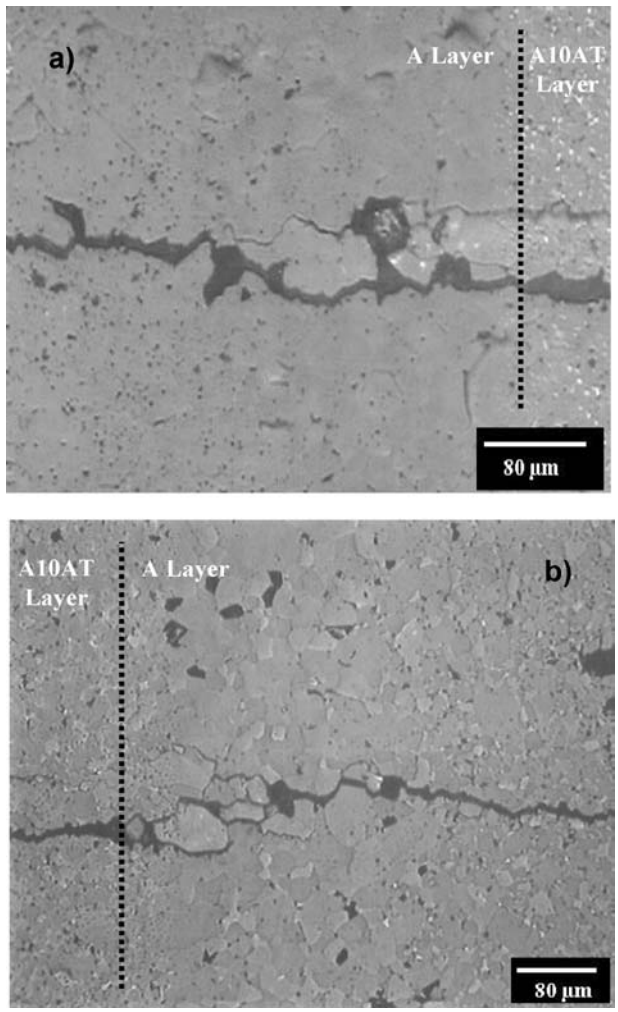

Figure 4 Characteristic features of the crack path in the notched samples of the laminate after testing. Crack growth direction is from left to right. Optical micrographs of polished lateral faces of the samples. (a) Crack branching when it reaches the grain sized alumina layer. The large alumina grains act as sites for crack branching and (b) Large alumina grains of the large grain sized alumina layers acting as bridges in the wake of the propagating crack.

that confer flaw tolerant behaviour to the laminates due to crack branching and bridging, can be formed during the thermal treatment starting from small grain sized green compacts and using the effect of TiO_2 in the microstructural development of alumina.

Acknowledgments

Work supported by the projects CICYT MAT2003-00836 and CAM GRMAT0707-2004, by the grant CSIC I3P-BPD2001-1, Spain, and in part by the European Community's Human Potential Programme under contract HPRN-CT-2002-00203, [SICMAC].

The WDS analyses were performed in Centro de Microscopía Electrónica, UCM, Madrid, and the standards supplied by Smithsonian Institute, Washington.

References

1. H. M. CHAN, *Annu. Rev. Mater. Sc.* **27** (1997) 249.

2. B. R. LAWN, N. P. PADTURE, L. M. BRAUN and S. J. BENNISON, *J. Am. Ceram. Soc.* **76** (1993) 2235.
3. N. P. PADTURE, J. L. RUNYAN, S. J. BENNISON, L. M. BRAUN and B. R. LAWN, *J. Am. Ceram. Soc.* **76** (1993) 2241.
4. S. BUENO, R. MORENO and C. BAUDÍN, *J. Eur. Ceram. Soc.* **24** (2004) 2785.
5. R. URIBE and C. BAUDÍN, *J. Am. Ceram. So.* **86** (2003) 846.
6. S. BUENO, R. MORENO and C. BAUDÍN, *J. Eur. Ceram. Soc.* **25** (2005) 847.
7. L. AN, H. M. CHAN, N. P. PADTURE and B. R. LAWN, *J. Mater. Res.* **11** (1996) 204.
8. L. AN, H. HA and H. M. CHAN, *J. Am. Ceram. Soc.* **81** (1998) 3321.
9. C. J. RUSSO, M. P. HARMER, H. M. CHAN and G. M. MILLER, *J. Am. Ceram. Soc.* **75** (1992) 3396.
10. J. D. POWERS and A. M. GLAESER, in "Sintering Technology" (Marcel Dekker Inc, New York, 1996) p. 33
11. B. FREUDENBERG and A. MOCELLIN, *J. Am. Ceram. Soc.* **70** (1987) 33.
12. P. L. SWANSON, C. J. FAIRBANKS, B. R. LAWN, Y. W. MAI and B. J. HOCKEY, *J. Am. Ceram. Soc.* **70** (1987) 279.
13. Y. KIM, S. HONG and D. KIM, *J. Am. Ceram. Soc.* **83** (2000) 2809.
14. R. L. FULLMANN, *Trans. AIME. Journ. of Metals* **197** (1953) 447.
15. H. SONG and R. L. COBLE, *J. Am. Ceram. Soc.* **73** (1990) 2077.
16. D. G. BRANDON, O. GLOZMAN, L. BAUM AND R. GRYLLS, in Proceedings of the Third Euro-Ceramics, Madrid, 1993, edited by P. Durán and J. F. Fernández (Faenza Editrice Ibérica S. L., 1993) p. 725.

Received 15 March
and accepted 03 August 2005